APPLIED ORGANOMETALLIC CHEMISTRY
Appl. Organometal. Chem. 2001; **15**: 833–840
DOI: 10.1002/aoc.237

Characterization of SiC and Si_3N_4 coatings synthesized by means of inductive thermal plasma from disilane precursors

E. Bouyer,* G. Schiller, M. Müller and R. H. Henne
Deutsches Zentrum für Luft-und Raumfahrt (DLR), Institut für Technische Thermodynamik, Pfaffenwaldring 38–40, 70569 Stuttgart, Germany

The synthesis of SiC (and/or Si_3N_4) in an inductive thermal plasma from liquid disilane precursor is described in this paper. One goal of the process presented hereafter is the valorization of a liquid disilane fraction, which is a by-product of the silicone industry. The liquid precursor is atomized in the core of the thermal inductive plasma and decomposed in the high-temperature zone. The coating grows on the substrate according to the thermal plasma chemical vapor deposition (CVD) process. The resulting synthesized materials are investigated by means of X-ray diffraction, scanning and transmission electron microscopy, and nuclear magnetic resonance. The composition of the material synthesized is studied as a function of process parameters, such as the plasma gas nature and its composition, the atomization gas flow rate and the plasma reactor pressure. Control over the composition of the synthesized material composition, as well as the coating microstructure, can be achieved by an appropriate adjustment of the experimental parameters. Nanostructured α/β-SiC and α/β-Si_3N_4 can be synthesized successfully with such a thermal plasma process. The deposition rate reached with such a technology is more than 20 $\mu m\ min^{-1}$, which is two to three orders of magnitude higher than that of the conventional CVD method. Copyright © 2001 John Wiley & Sons, Ltd.

Keywords: disilane; SiC; Si_3N_4; inductively coupled plasma; coating; synthesis

Received 15 March 2000; accepted 10 September 2000

* Correspondence to: E. Bouyer, Deutsches Zentrum für Luft-und Raumfahrt (DLR), Institut für Technische Thermodynamik, Pfaffenwaldring 38–40, 70569 Stuttgart, Germany.
Email: etienne.bouyer@dlr.de
Contract/grant sponsor: Deutsche Forschungsgemeinschaft.

INTRODUCTION

Advanced non-oxide silicon-based materials, such as SiC, are commonly produced by inorganic solid-state reactions carried out at high temperature. Industrially, SiC is synthesized in large amounts through the reaction of silica with carbon according to the Acheson process at $2200 < T < 2500$ °C.[1] Since the mid 1970s, it has been known that SiC can be produced at unusually low temperatures (800–1200 °C) by the thermal decomposition of organo-silicon preceramic polymers.[2] A broad range of such polymer or oligomer precursors is now available for a wide range of ceramic phase syntheses,[3,4] as well as for composite ceramic materials.[5] One of these precursors, the group of chlorinated silane compounds, has been extensively studied for SiC synthesis. Its decomposition starts at 700 °C and finishes at 1300 °C; the chlorine disappearance starts at 1000 °C and finishes at temperatures higher than 1800 °C.[6] In the temperature range between 700 and 800 °C silanes are transformed into amorphous silicon carbide, which crystallizes above 1100 °C. After a pyrolysis process above 1500 °C only silicon carbide exists.[7]

Ceramic phases containing SiC/Si_3N_4 can also be synthesized by means of a broad range of techniques, from pyrolysis (followed by sintering)[8] for bulk material preparation to chemical vapor deposition (CVD) as a coating process. This latter technique is restricted to thin coatings deposition. Therefore, simultaneous synthesis and deposition of SiC/Si_3N_4 can be achieved by vapor-phase methods with a relatively low substrate temperature using improved CVD methods, like plasma-enhanced CVD (PECVD) or plasma-assisted CVD (PACVD).[9–11] These techniques are activated (or assisted) by a non-equilibrium plasma, either a radio-frequency (rf) or a microwave plasma. However, the deposition rate of these ceramic materials, even when applying such CVD methods, is still relatively low (a few micrometers per hour).[12]

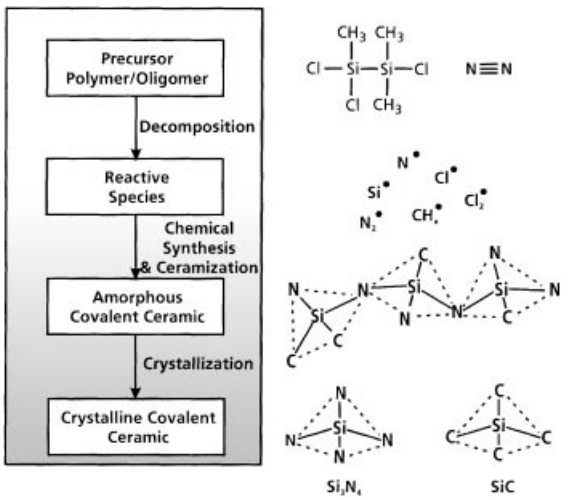

Figure 1 Flow chart for the SiC–Si_3N_4 plasma synthesis.

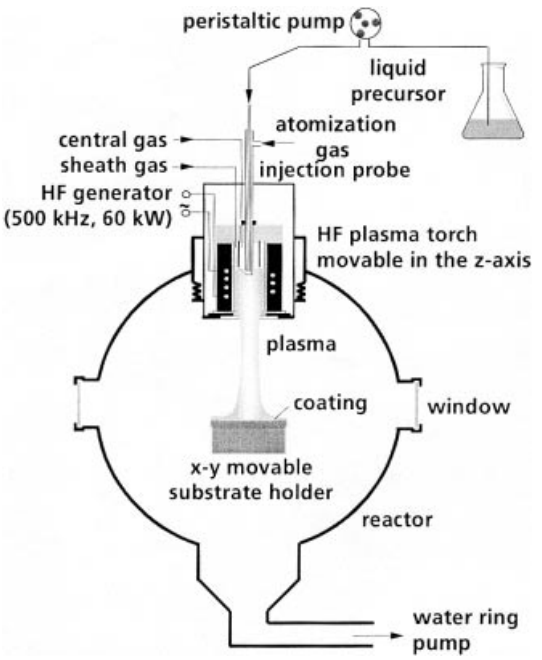

Figure 2 Rf induction plasma installation.

In the late 1980s, Murakami *et al.*[13] and Pfender *et al.*[14] simultaneously implemented the thermal plasma CVD (TPCVD) process, also called thermal plasma spray pyrolysis, in which a liquid (a solution of inorganic or organic salts) is injected into an inductively coupled plasma; the liquid then reacts in the plasma to form a product that condenses on a substrate with a relatively high deposition rate compared with the classical CVD method, i.e. three orders of magnitude faster.[15] The high deposition rate can be attributed to the high density of clusters formed at elevated pressure (close to 1 atm) and to the large volume of gaseous or liquid reactants that can be excited in an rf plasma.[16] In addition, owing to the electrodeless rf plasma generation, this method combines high deposition rate and clean chemistry. This paper presents a novel one-step ceramic coating synthesis route through the high-temperature decomposition of a organosilicon liquid precursor. This TPCVD process uses the inductive thermal plasma both as a heating source and as a reaction medium. Hence the plasma acts as a chemical reactor (plug flow reactor) with a reactant dwell time of less than a few tens of milliseconds. The elementary steps that take place during the plasma treatment are described in the flow chart in Fig. 1. The disilane mixture precursor is a low-cost by-product coming from the Müller–Rochow synthesis in the silicone industry.[17] The process is applied to the SiC and/or Si_3N_4 synthesis. The resulting coating materials are fully investigated in order to study the effect of the experimental parameters, such as the atomization gas flow rate, the hydrogen (or nitrogen) content in the plasma sheath gas, the reactor pressure, the spray distance (defined as the distance between the substrate surface and the bottom of the inductive torch) and the precursor composition.

EXPERIMENTAL

TPCVD experiments are carried out in a soft vacuum plasma reactor, depicted schematically in Fig. 2. Details concerning the TPCVD process of SiC can be found elsewhere.[18] The disilane fraction precursor used as raw material in this work is a chlorodisilane (CDS) fraction. The fraction was provided by Vecur e.V. (Freiberg, Germany); its composition is summarized in Fig. 3.

The experimental conditions for silicon-based ceramic materials synthesis and deposition are listed in Table 1. Molybdenum plates ($40 \times 40 \times 3\ mm^3$) are used as the substrate, which can be cooled during the deposition process.

The coating morphology was studied by means of a Topcon DS 130 scanning electron microscope (SEM). Phase analysis by X-ray diffraction (XRD) pattern was carried out by means of a STOE diffractometer.[29] Si magic angle spinning (MAS)

Table 1 Experimental conditions

	SiC synthesis	Si_3N_4 synthesis
Plasma gas flow rate (slpm)[a]		
central	15	
sheath	60/5–60/10 Ar/H_2	60/10–10/50 Ar/N_2
atomization	5–10 Ar	
Disilane injection rate (ml min^{-1})	3	
Rf power (KW)	28–35	
Spray distance (mm)	100–2040	
Reactor pressure (kPa)	20–40	
Experiment duration (s)	120–300	

[a] slpm: standard liters per minute.

nuclear magnetic resonance (NMR) spectra were recorded on a Bruker MSL 300 (59.3 MHz). Transmission electron microscope (TEM) pictures analysis was performed on a Zeiss EM 912 Ω operated with 120 kV. For the TEM imaging, the conventional bright field (BF) mode was used.

RESULTS AND DISCUSSION

SiC synthesis

Most of the SiC synthesis experiments were been performed with hydrogen as the secondary plasma sheath gas. Figure 4 shows the XRD patterns corresponding to two experimental conditions, namely (a) 10 slpm hydrogen and (b) 5 slpm hydrogen as the secondary plasma sheath gas flow rate, and performed with a non-cooled molybdenum substrate. The diffraction peaks are all assigned to the β-phase of SiC. Addition of hydrogen in a plasma improves substantially the transport properties of the plasma and thus the heat transfer between plasma and the material to be treated,[19] namely the disilane spray. An increase in the hydrogen plasma gas content leads to an increase in crystallinity of the β-SiC coating. These experimental conditions are the more favorable for the synthesis of high crystallinity β-SiC coatings, owning to the combination of the high hydrogen content, the high substrate temperature and the relatively high spray distance (200 mm). The TEM picture of a crushed SiC sample shows a typical grain of 200 nm in size; see Fig. 5. Figure 6 shows

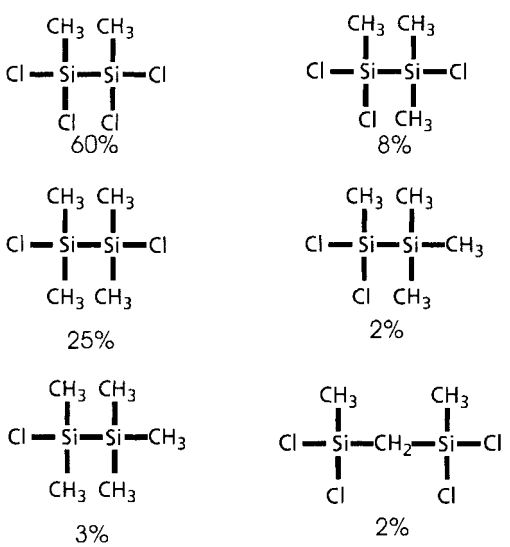

Figure 3 Composition of the CDS fraction, in mole percent.

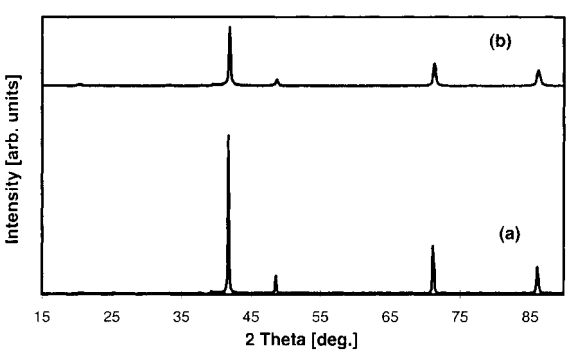

Figure 4 XRD pattern of as-deposited SiC coating: (a) plasma power level: 35 kW; pressure: 20 kPa; plasma gas composition: Ar/H_2 60/10 slpm; 5 slpm Ar atomization gas; spray distance: 200 mm; deposition time: 300 s; (b) plasma power level: 35 kW; pressure: 20 kPa; plasma gas composition: Ar/H_2 60/5 slpm; 5 slpm Ar atomization gas; spray distance: 200 mm; deposition time: 300 s.

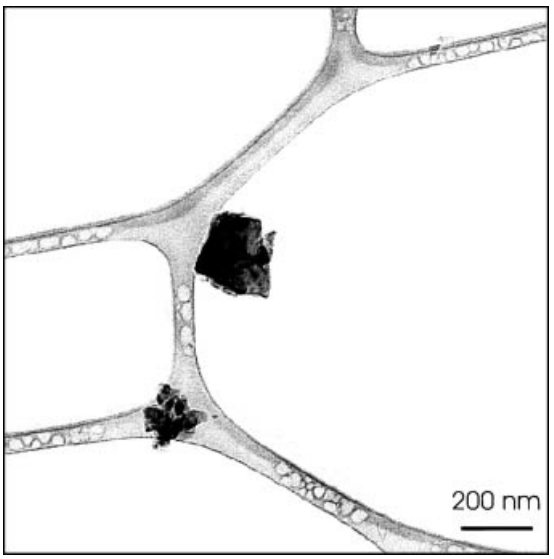

Figure 5 TEM picture (BF) of as-synthesized SiC (plasma power level: 30 kW; pressure: 20 kPa; plasma gas composition: Ar/H_2 60/5 slpm; 5 slpm Ar atomization gas; spray distance: 200 mm; deposition time: 120 s).

an SEM picture of a fractured SiC coating that is relatively dense and which was prepared with a 20 $\mu m\ min^{-1}$ deposition rate.

For comparison with Fig. 4, Fig. 7 shows an XRD pattern of a sample obtained with the opposite experimental conditions, namely a low hydrogen content, a short spray distance (150 mm) and a

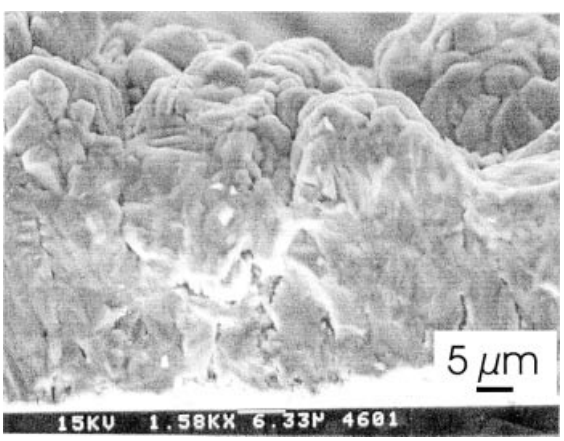

Figure 6 SEM picture (secondary electron, SE) of an SiC fractured coating (plasma power level: 32 kW; pressure: 20 kPa; plasma gas composition: Ar/H_2 60/5 slpm; 10 slpm Ar atomization gas; spray distance: 200 mm; deposition time: 140 s).

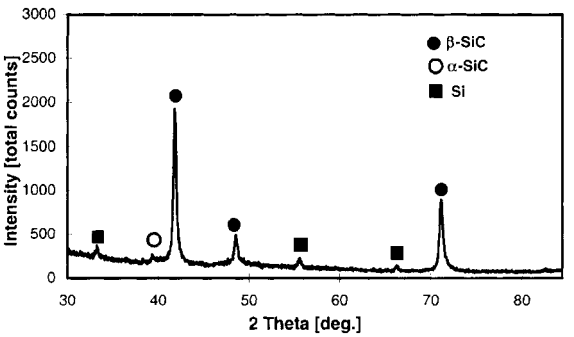

Figure 7 XRD pattern of as-deposited SiC coating (plasma power level: 28 kW; pressure: 30 kPa; plasma gas composition: Ar/H_2 60/5 slpm; 10 slpm Ar atomization gas; spray distance: 150 mm; deposition time: 180 s).

moderate substrate temperature (molybdenum plate fixed on a water-cooled substrate holder). In addition to β-SiC, the presence of α-SiC and free silicon can be noticed. The coating is nanostructured, since the crystallite size calculated with the Scherrer equation (corrected by the subtraction of the instrumental peak broadening)[20,21] on the basis of the (111) β-SiC diffraction peak gives 27 nm. The TEM picture obtained from this sample (after crushing of the coating) shows fine grains smaller than 50 nm surrounded by big agglomerates (Fig. 8)

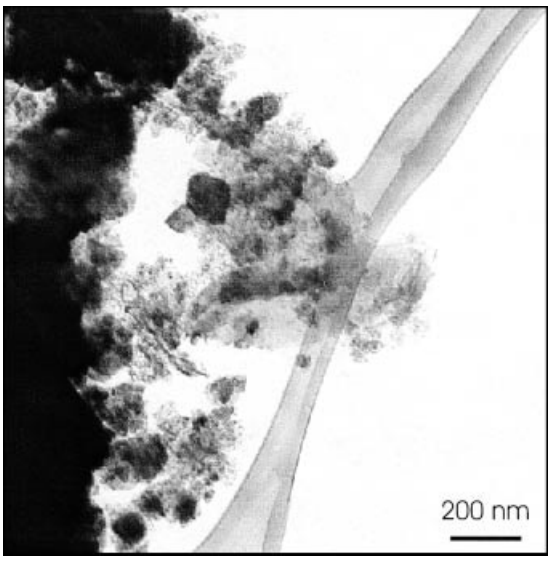

Figure 8 TEM picture (BF) of as-synthesized SiC (plasma power level: 28 kW; pressure: 30 kPa; plasma gas composition: Ar/H_2 60/5 slpm; 5 slpm Ar atomization gas; spray distance: 150 mm; deposition time: 300 s).

and is in good agreement with the calculated crystallite size.

Hydrogen promotes the decomposition and reduction of silane to produce more silicon nuclei (or clusters).[22] The dimethyltetrachlorodisilane is the main phase contained in the CDS fraction; see Fig. 3. The following reaction mechanism is proposed:

$$(CH_3)_2Si_2Cl_4 + 3H_2 \Leftrightarrow 2Si + 2CH_4 + 4HCl \quad [1]$$

$$CH_4 \Leftrightarrow C + 2H_2 \quad [2]$$

$$Si + C \Leftrightarrow SiC \quad [3]$$

Previous work from Huang *et al.* has shown that the reaction rate of Eqn [1] is higher than that of Eqn [2] in the normal pyrolysis temperature range.[23] Moreover, addition of hydrogen in the plasma sheath gas will slow down the reaction in Eqn [2] according to the Le Chatelier principle. In accordance with the reaction in Eqn [3] residual silicon is also found. This suggests that homogeneous nucleation of silicon particles from the supersaturated silicon vapor is the first step in the SiC synthesis process. Therefore, owing to the small size of the silicon particles (stable cluster) formed under thermal plasma conditions, a large specific surface area is obtained for the heterogeneous chemical reaction to occur, coupled with the further diffusion of carbon into the volume of the particle through the SiC shell. Even if the diffusion within the already condensed phase is a time-dependent (and temperature-dependent) process—for a 2 nm diameter silicon particle the central atom is located only about three atoms from the surface—then at this short scale the diffusion can start in the plasma plume and finish on the substrate when its temperature is high enough. Previous work has led to the same conclusion concerning the SiC nucleation process.[24,25] The presence of free silicon, i.e. non-reacted silicon, in some attempts (low reactor pressure, low spray distance implies low residence time; low substrate temperature) suggests that the silicon nucleation occurs first and that the unreacted silicon consumption cannot be completed even with a favorable atomic C/Si ratio (C/Si = 1.35). Carbon diffusion through SiC and carbon reaction with free silicon are the limiting steps of this process. In most of the XRD patterns, free carbon is not detected owing to its insignificant presence and its amorphous nature.

The substitution of hydrogen by nitrogen in the secondary plasma sheath gas gives a quite different result. With a comparable plasma power level the resulting material has a lower crystallinity associated with a crystallite size of 14 nm. Moreover, it is worth noticing on the XRD pattern that the sample contains mainly α-SiC (6H and 4H polytypes); Fig. 9. In the NMR spectrum shown in Fig. 10 one can observe a 'mountain-like' signal representing the SiC phase[26] (−18.6 ppm) associated with another small signal (−46.0 ppm), which can be assigned to SiN_4 environments. The relatively high chemical shift may be attributed to the nanocrystalline structure resulting from such experimental conditions. NMR, which is a local

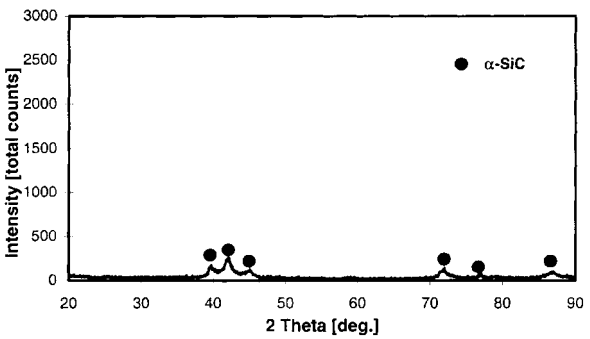

Figure 9 XRD pattern of as-deposited SiC coating (plasma power level: 28 kW; pressure: 30 kPa; plasma gas composition: Ar/N_2 60/10 slpm; 5 slpm Ar atomization gas; spray distance: 150 mm; deposition time: 300 s).

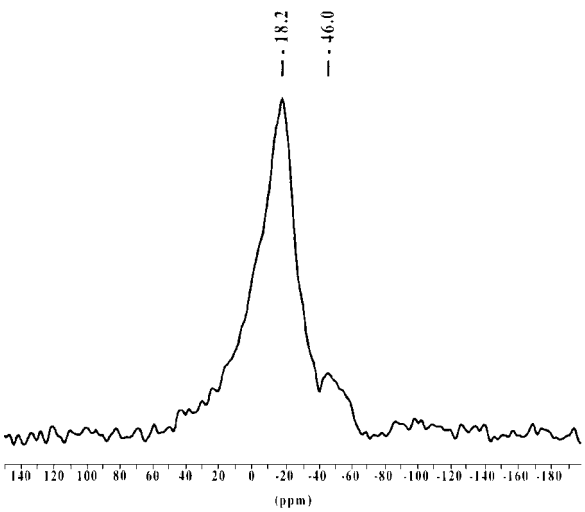

Figure 10 ^{29}Si MAS-NMR spectra of as-synthesized SiC (plasma power level: 28 kW; pressure: 30 kPa; plasma gas composition: Ar/N_2 60/10 slpm; 5 slpm Ar atomization gas; spray distance: 150 mm; deposition time: 300 s).

analytical technique, has detected the start of the silicon nitride formation, which is not detectable by means of XRD. This is probably due to the presence of amorphous Si_3N_4 as secondary phase. Nitrogen has a thermal effect during the plasma treatment; unlike hydrogen, addition of nitrogen does not increase the plasma transport properties as much in the operating temperature range. It is well established that the thermal efficiency, in terms of heat transfer, of a nitrogenated plasma is not as efficient as a hydrogenated plasma. The second effect of nitrogen induces a delay in crystallization. As mentioned by Monthioux and Delverdier[27] and Kurtenbach *et al.*,[28] heteroatoms like oxygen or nitrogen inhibit the SiC crystal nucleation.[27,28] A slightly nitrogenated plasma seems to block the crystallization of the SiC coating.

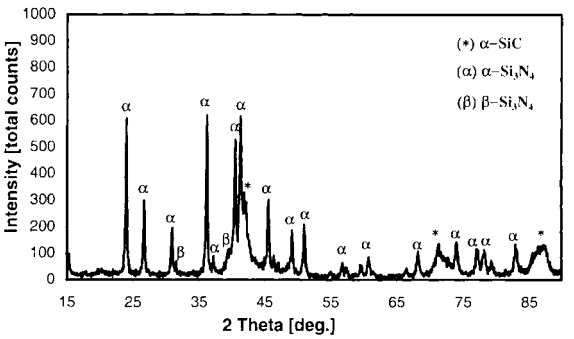

Figure 11 XRD pattern of as-deposited Si_3N_4 coating (plasma power level: 33 kW; pressure: 20 kPa; plasma gas composition: Ar/N_2 10/50 slpm; 5 slpm Ar atomization gas; spray distance: 200 mm; deposition time: 120 s).

Silicon nitride synthesis

In order to prepare silicon nitride from the precursor applied, the plasma should contain a nitriding agent such as ammonia or nitrogen. Nitrogen is a poor nitriding agent, in comparison with ammonia, due to the relatively high chemical stability of nitrogen at high temperature. However, in this study nitrogen was used since it is easier to handle than ammonia. A larger amount of nitrogen is needed to achieve the same nitriding effect as with ammonia. Most of the literature dealing with Si_3N_4 synthesis under thermal plasma conditions reports experiments performed with ammonia as nitriding agent.[29] Ammonia is generally injected radially downstream of the torch exit. In the present study nitrogen is injected axially as a forming and reactive gas, since nitrogen is a part of the plasma sheath gas. For this purpose, a few attempts were carried out with a high nitrogen plasma gas content (50 slpm) and with a non-cooled substrate. One can notice from the XRD pattern in Fig. 11 that a mixture of α- and β-Si_3N_4 is synthesized, with α-Si_3N_4 as the major phase and with broad diffraction peaks assigned to α-SiC. The corresponding NMR spectrum shows two overlapping peaks that form a narrow signal; see the enlarged area in Fig. 12 ($\delta_{^{29}Si} = -46.8$ and -48.9 ppm). The two signals may be attributed to α-Si_3N_4; this is in good agreement with the XRD pattern. The second peak ($\delta_{^{29}Si} = -17.1$ and -20.8 ppm) is assigned to α-SiC.[30] The peak width in the NMR spectrum is consistent with the nanocrystalline structure of the SiC phase.

A similar Si_3N_4 synthesis experiment has been performed where the atomization gas flow rate was raised from 5 to 10 slpm of argon. A higher atomization flow rate leads to a smaller mean droplet size,[31] since the ratio 'atomization gas flow rate/liquid flow rate' governs the resulting droplet size distribution.[32] The XRD pattern of this attempt shows a mixture α/β-Si_3N_4 with β-Si_3N_4 as the main component; Fig. 13. The SEM picture representing a coating top view, see Fig. 14(b), shows a 'coating' consisting of isolated fibers that have grown perpendicularly to the substrate surface. However, these 'match fibers' are formed by smooth fibers terminated with an equiaxed microstructure, which may be attributed to the α-phase. A

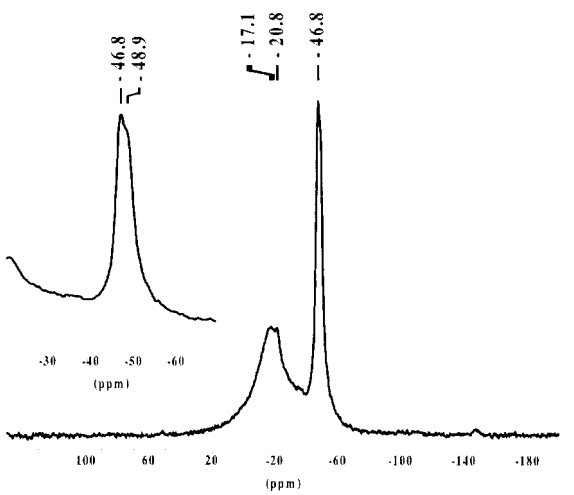

Figure 12 ^{29}Si MAS-NMR spectrum of as-synthesized Si_3N_4 (plasma power level: 33 kW; pressure: 20 kPa; plasma gas composition: Ar/N_2 10/50 slpm; 5 slpm Ar atomization gas; spray distance: 200 mm; deposition time: 120 s).

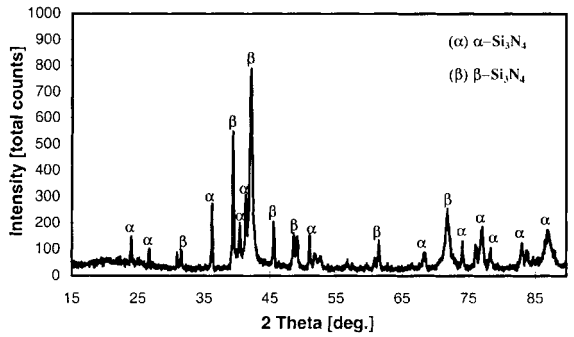

Figure 13 XRD pattern of as-deposited Si_3N_4 coating (plasma power level: 33 kW; pressure: 20 kPa; plasma gas composition: Ar/N_2 10/50 slpm; 10 slpm Ar atomization gas; spray distance: 200 mm; deposition time: 120 s).

reduced atomization gas pressure promotes the synthesis and deposition of α-Si_3N_4 as a dense coating with an equiaxed microstructure; Fig. 14(a).

By way of comparison, reaction-bonded silicon nitride, which is formed by reaction between silicon powder compacts and nitrogen gas at high temperature, is equiaxed in grain structure and primarily made up of the α-phase.[33] In the present process, as already discussed in the previous subsection, silicon nitride and carbide are formed by nitridation and carburization respectively of silicon clusters already nucleated in plasma conditions. One can assume that the α-phase, which is the less stable of the two phases at high temperature, is more likely to be synthesized with a shorter dwell time of the reactants in the plasma zone (bigger disilane droplet size), whereas the acicular structure (the β-phase) is formed preferentially during longer dwell times. More investigations will be devoted to the characterization of the different parts of the fibers. Recent investigations are devoted to the characterization of the different parts of the fibers and will be published elsewhere.

CONCLUSIONS

SiC and/or Si_3N_4 coatings associated with a variety of possible microstructures have been synthesized by inductive thermal plasma spray pyrolysis/TPCVD. The coating deposition rate reaches 20 μm min^{-1}. The results of this work support the mechanism in which homogeneous nucleation of silicon is the first step in both the SiC and Si_3N_4 syntheses prior to the following carburization and nitridation processes respectively. Key process parameters have been identified: the residence time of the precursors (which depends on the spray distance and on the plasma stream velocity), the droplets size distribution (controlled by the ratio of atomization gas flow rate/disilane flow rate), the substrate temperature, and the heat transfer effi-

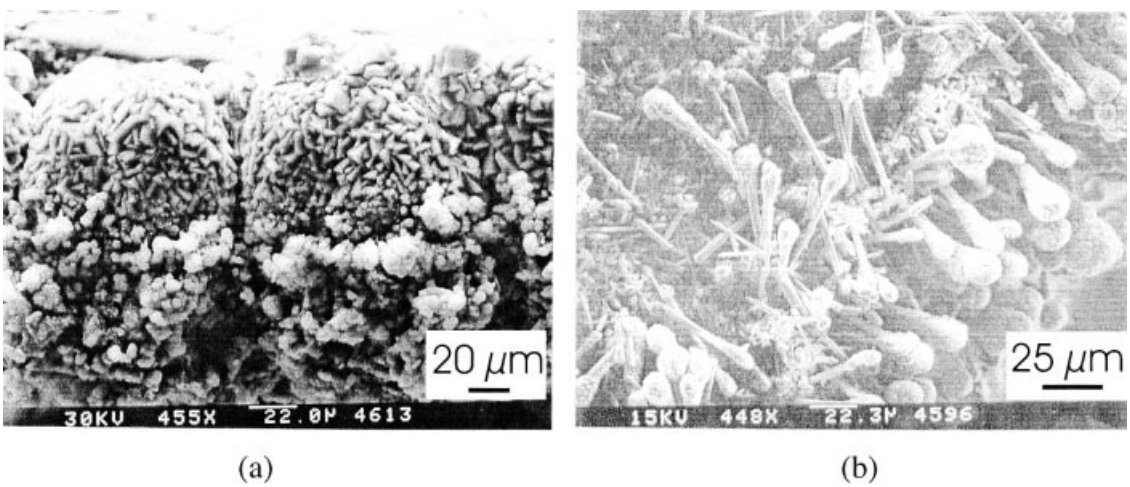

Figure 14 SEM picture (SE) of as-deposited Si_3N_4 coating (a) plasma power level: 35 kW; pressure: 20 kPa; plasma gas composition: Ar/H_2 60/10 slpm; 5 slpm Ar atomization gas; spray distance: 200 mm; deposition time: 120 s; (b) plasma power level: 35 kW, pressure: 20 kPa, plasma gas composition: Ar/H_2-60/5 slpm, 10 slpm Ar atomization gas, spray distance: 200 mm, deposition time: 120 s.

ciency (depending on the plasma gas nature). The control of these parameters permits one to synthesize a broad range of materials with different structures from nanomaterials to bulk materials. Further work will be directed towards the reactive suspension plasma spraying of disilane mixed with solid additives (e.g. B_4C, Al_2O_3, titanium, …). This will open the way to synthesize materials like Si–C–B–N, Sialons, and Si–C–Ti–N from a cost-effective disilane precursor, as was used in this study.

Acknowledgements The work has been supported financially by the Deutsche Forschungsgemeinschaft (DFG). The authors would like to acknowledge the technical assistance and the helpful discussions on solid-state NMR with Dr E. Brendler from the Institute for Analytical Chemistry at Freiberg University of Mining and Technology (Germany). Thanks to Dr A. Zern from the Max Planck Institute for Metallurgy (Stuttgart, Germany) for the TEM investigations and to Dr K. Trommer from Vecur e.V. (Freiberg, Germany) for providing the disilane precursors.

REFERENCES

1. Reed JS. *Ceramics Processing*, 2nd edn. John Wiley and Sons Inc.: New York, 1995; 35–53.
2. Yajima S, Hayashi J, Omori M, Okamura K. *Nature* 1976; **261**: 683.
3. Aldinger F, Weinmann M, Bill J. *Pure Appl. Chem.* 1998; **70**: 439.
4. Müller E, Martin HP. *J. Prakt. Chem.* 1997; **339**: 401.
5. Chew KW, Sellinger A, Laine RM. *J. Am. Ceram. Soc.* 1999; **82**: 857.
6. Martin HP, Müller E, Brendler E. *J. Mater. Sci.* 1996; **31**: 4363.
7. Martin HP, Irmer G, Schuster G, Müller E. *Fresenius' J. Anal. Chem.* 1994; **349**: 160.
8. Riedel R, Seher M, Mayer J, Szabó DV. *J. Eur. Ceram. Soc.* 1995; **15**: 703.
9. Gerretsen J, Kirchner G, Kelly T, Mernagh V, Koekoek R, McDonnell M. *Surf. Coat. Technol.* 1993; **60**: 566.
10. Lelogeais M, Ducarroir M. *Surf. Coat. Technol.* 1991; **48**: 121.
11. Kim HS, Park YJ, Choi IH, Baik YJ. *Thin Solid Films* 1999; **341**: 42.
12. Smith DL. *Thin-Film Deposition: Principles & Practice*. McGraw-Hill: 1995.
13. Murakami H, Yoshida T, Akashi K. *Adv. Ceram. Mater.* 1988; **3**(4): 423.
14. Pfender E, Zhu H, Lau YC. *Mater. Sci. Eng.* 1991; **139**: 352.
15. Yoshida T. *Pure Appl. Chem.* 1994; **6**: 1223.
16. Lu SP, Heberlein J, Pfender E. *Plasma Chem. Plasma Process.* 1992; **12**: 35.
17. Rochow EG. *An Introduction to the Chemistry of the Silicones*, 2nd edn. John Wiley & Sons Inc.: London, 1951; 141–159.
18. Bouyer E, Müller M, Schiller G, Henne R. Conversion of silanes into SiC by RF plasma technology. In *Proc. of UTSC'99*, Düsseldorf, 15–19 March, 1999; 853–858.
19. Boulos MI, Fauchais P, Pfender E. *Thermal Plasmas, Fundamentals and Applications*, vol. 1. Plenum Press: New York, 1994; 213–323.
20. Cullity BD. *Elements of X-Ray Diffraction*, 2nd edn. Addison-Wesley: Reading, MA, 1978; 99–106.
21. Eberhart JP. *Structural and Chemical Analysis of Materials: X-Ray, Electron and Ion Spectrometry*. Wiley: New York, 1994; 576p.
22. Zhu CW, Zhao GY, Revankar V, Hlavacek V. *J. Mater. Sci.* 1993; **28**: 659.
23. Huang ZR, Laing B, Jiang DL, Tan SH. *J. Mater. Sci.* 1996; **31**: 4327.
24. Rao N, Girshick S, Heberlein J, McMurry P, Jones S, Hansen D, Micheel B. *Plasma Chem. Plasma Process.* 1995; **15**: 581.
25. Carmer CS, Frenklach M. *Appl. Phys. Lett.* 1989; **54**: 1430.
26. Martin HP, Müller E, Irmer G, Babonneau F. *Fresenius' J. Eur. Ceram. Soc.* 1997; **17**: 659.
27. Monthioux M, Delverdier O. *J. Eur. Ceram. Soc.* 1996; **16**: 721.
28. Kurtenbach D, Martin HP, Müller E, Roewer G, Hoell A. *J. Eur. Ceram. Soc.* 1998; **18**: 1885.
29. Soucy G, Jurewicz JW, Boulos MI. *J. Mater. Sci.* 1995; **30**: 2008.
30. Guth JR, Petuskey WT. *J. Phys. Chem.* 1987; **91**: 5361.
31. Bouyer E, Schiller G, Müller M, Henne R. *Plasma Chem. Plasma Process*. 2000; **21**: 523.
32. Lavernia E, Wu Y. *Spray Atomization and Deposition*. John Wiley & Sons: Chichester, 1996; 49–153.
33. Chiang YM, Birnie D, Kingery WD. *Physical Ceramics, Principles for Ceramic Science and Engineering*. John Wiley and Sons Inc.: New York, 1997; 19–72.

